

Giant Spin-splitting in the Bi/Ag(111) Surface Alloy

Christian R. Ast,^{1,2} Daniela Pacil ,¹ Mihaela Falub,¹ Luca Moreschini,¹ Marco Papagno,¹
Gero Wittich,² Peter Wahl,² Ralf Vogelgesang,² Marco Grioni,¹ and Klaus Kern^{1,2}

¹Ecole Polytechnique F d rale de Lausanne (EPFL), Institut de Physique des Nanostructures, CH-1015 Lausanne, Switzerland

²Max-Planck-Institut f r Festk rperforschung, 70569 Stuttgart, Germany

Surface alloying is shown to produce electronic states with a very large spin-splitting. We discuss the long range ordered bismuth/silver(111) surface alloy where an energy bands separation of up to one eV is achieved. Such strong spin-splitting enables angular resolved photoemission spectroscopy to directly observe the region close to the band edge, where the density of states shows quasi-one dimensional behavior. The associated singularity in the local density of states has been measured by low temperature scanning tunneling spectroscopy. The implications of this new class of materials for potential spintronics applications as well as fundamental issues are discussed.

PACS numbers: 73.20.At,71.70.Ej,68.37.Ef,79.60.-i

Manipulating the electron spin without employing magnetic fields is a vision that lies at the heart of spintronics. The spin-orbit (SO) interaction — which couples orbital and spin degrees of freedom — provides the basis for spin manipulation by means of electric fields. It plays a vital role in various device proposals in spin-based quantum information technology [1, 2, 3, 4]. One proposal for a spin transistor [2], for example, relies on the spin-precession of a propagating electron due to a SO-induced spin splitting [5, 6]. However, external electric fields are typically not strong enough to induce an appreciable phase shift within the electron’s mean free path. Internal electric fields, e. g. induced by spacial inversion asymmetry, are much stronger, yet the spin-splitting in semiconductors, which are the materials of choice in spintronics, is smaller than what is found for metallic surface states [7].

Clean surfaces of elemental metals show a trend of strong atomic spin-orbit coupling leading to a large spin-splitting of their surface states, which can be further enhanced by the adsorption of adatoms [8, 9, 10]. This is a promising path to create a new class of nanoscale structures where morphology and chemistry are used to tune the spin-splitting of interface states. Surface alloying in particular provides interesting opportunities as the adatoms *replace* substrate atoms of the topmost monolayer in their lattice sites creating a new two-dimensional electronic structure.

In this report we demonstrate that the band structure of the bismuth/silver surface alloy grown on a Ag(111) substrate exhibits a giant spin splitting. Angular-resolved photoemission spectroscopy (ARPES) has been employed to map the characteristically offset parabolic bands. This large splitting offers experimental access to a region near the band maximum where the density of states diverges and the spin orientation changes its sense of rotation. Low temperature scanning tunneling microscopy/spectroscopy (STM/STS) has been employed to study the topography and the local density of states (LDOS) of the alloy. A distinct peak in the measured LDOS shows, as predicted by theory, the quasi one-dimensional van Hove singularity at the band edge. This introduces an experimental approach for identifying spin splitting by STS.

The ARPES measurements were done at room temperature and LN2 (77 K) temperatures using 21.2 eV photons (HeI) in ultra-high vacuum ($2 \cdot 10^{-10}$ mbar). Sample preparation was

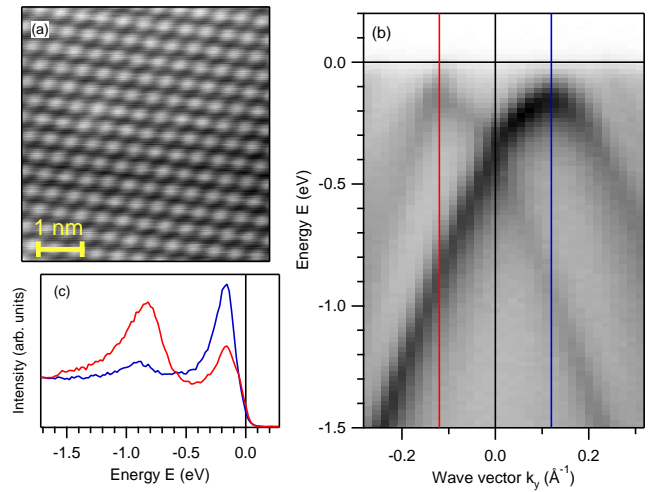


FIG. 1: (color online) (a) Topography by STM of the long-range ordered Bi/Ag(111) surface alloy (Bias voltage: -3 mV; Tunneling current: 1 nA). The alloy is grown in ultra-high vacuum by depositing one third of a monolayer of bismuth onto a clean Ag(111) surface at a temperature of 400 K to yield a $\sqrt{3} \times \sqrt{3}R30^\circ$ reconstruction. (b) ARPES band structure image near the $\bar{\Gamma}$ -point, i. e. the center of the surface Brillouin zone, showing the spin-split bands of the Bi/Ag(111) surface alloy. The intensity scale is linear with light and dark areas corresponding to low and high intensity, respectively. (c) Energy distribution curves to the left and right of the $\bar{\Gamma}$ -point as indicated by the respective lines in (b).

done *in situ*. The energy and angular resolution of the analyzer were better than 10 meV and $\pm 0.015 \text{  }^{-1}$. The light is partially polarized with the polarization vector within a mirror symmetry plane perpendicular the (111) surface of the crystal. Photoelectrons were collected within the mirror plane for the geometry of Fig. 1. The STM/STS measurements were done at 6 K in ultra-high vacuum ($1 \cdot 10^{-10}$ mbar) with *in situ* sample transfer and preparation.

Figure 1(a) shows a topographic scan of the long-range ordered hexagonal surface alloy (5   lattice constant) taken by STM. Bright spots correspond to Bi atoms, each of which is surrounded by six Ag atoms, as indicated by the model in the

inset. Structural details will be published elsewhere. The corresponding band structure measured by ARPES near the $\bar{\Gamma}$ -point at the center of the surface Brillouin zone (SBZ) (Fig. 1(b)) shows two identical and nearly parabolic bands with negative effective mass. They replace the nearly free electron-like surface state of the bare Ag(111) surface and accommodate the p -electrons donated by the Bi atoms. Remarkably, their maxima are shifted to the left and right of $\bar{\Gamma}$. The offset k_0 increases from 0.12 \AA^{-1} at room temperature to 0.16 \AA^{-1} at liquid nitrogen temperatures (77 K), which is about 22 % of the SBZ.

The band on the right exhibits higher intensity. To better visualize this effect Fig. 1(c) shows two energy distribution curves to the left and right of $\bar{\Gamma}$. This asymmetry is the result of the parity of the electronic wave functions combined with the (linear) polarization of the exciting beam [5]. The observation of two symmetrically offset bands with an asymmetric distribution of intensities is, as for the surface state of the clean Au(111) surface [11], a clear indication of spin-orbit induced spin-splitting.

These observations can be qualitatively understood on the basis of a simple nearly free electron model. The Hamiltonian describing the spin-orbit coupling at the surface is [5, 12]:

$$H_{\text{SOC}} = \alpha(\vec{e}_z \times \vec{k}) \cdot \vec{\sigma}$$

where α is proportional to an effective electric field. The vector \vec{e}_z is perpendicular to the surface and $\vec{k} = (\vec{k}_{\parallel}, k_{\perp})$ is the electron wave vector, with components parallel and perpendicular to the surface. The energy dispersion is:

$$E(\vec{k}_{\parallel}) = \frac{\hbar^2}{2m^*}(k_{\parallel} - k_0)^2 + E_0$$

where m^* is the effective mass, k_0 is the offset by which the parabola is shifted away from $\bar{\Gamma}$ and a function of α . E_0 is an offset in energy. The energy dispersion is rotationally symmetric; it only depends on the magnitude of \vec{k}_{\parallel} .

The energy dispersion near $\bar{\Gamma}$ is visualized (energy vs. wave vector k_x and k_y) in the left panels of Fig. 2(a)-(c). The right panels show a set of experimental band structure images. Fig. 2(a) shows a cut through the center of the Brillouin zone. The bands cross at $\bar{\Gamma}$ and reach their maxima at $\pm k_0$ near the edges of the measured images. Away from $\bar{\Gamma}$ along the k_y -axis (Fig. 2(b)), the bands no longer cross. The upper band is rather flat while the lower band disperses with a parabola-like shape. In Fig. 2(c), at $k_y = 0.18 \text{ \AA}^{-1}$, beyond the band maximum, both bands show a parabola-like dispersion with a separation in energy of 935 meV!

Two qualitatively different energy regions can be identified which are detailed in Fig. 3(a). Region I reaches from the band maximum to the crossing of the two inner branches; region II reaches from this crossing point to lower energies. The main difference between these region concerns the density of states $D(E)$, which is easily evaluated analytically:

$$D(E) = \int \delta(E - E(\vec{k}_{\parallel})) \frac{d\vec{k}_{\parallel}}{4\pi^2} =$$

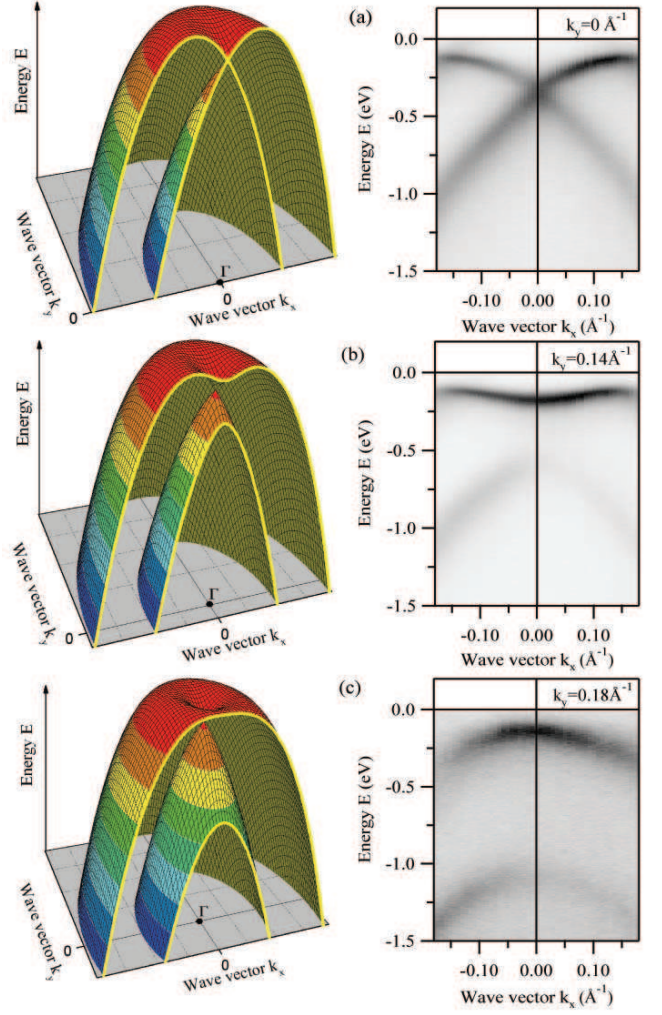


FIG. 2: (color online) (a)-(c) Calculated energy dispersion in the nearly free electron model (left) and experimental band structure images at different positions in k -space (right). The cuts are perpendicular to the image in Fig. 1(c) which leads, for our experimental geometry, to a homogeneous intensity distribution over the two branches. The yellow lines in the calculation correspond to the measured section.

$$= \begin{cases} \frac{|m^*|}{\pi\hbar^2} \frac{k_0}{\sqrt{2m^*(E - E_0)/\hbar^2}} & ; E \in \text{Region I} \\ \frac{|m^*|}{\pi\hbar^2} & ; E \in \text{Region II} \\ 0 & ; \text{elsewhere} \end{cases}$$

The density of states (DOS) in Fig. 3(b) is constant in region II like in the two-dimensional free electron model without spin-orbit splitting. In region I it follows a $1/\sqrt{E}$ -behavior reminiscent of the van Hove singularity in one-dimensional models. At the band maximum the DOS diverges and then drops to zero. This is a signature of the spontaneous symmetry breaking which occurs for any finite k_0 turning the two-dimensional point-like band maximum for $k_0 = 0$ into a quasi-one-dimensional ring-like maximum.

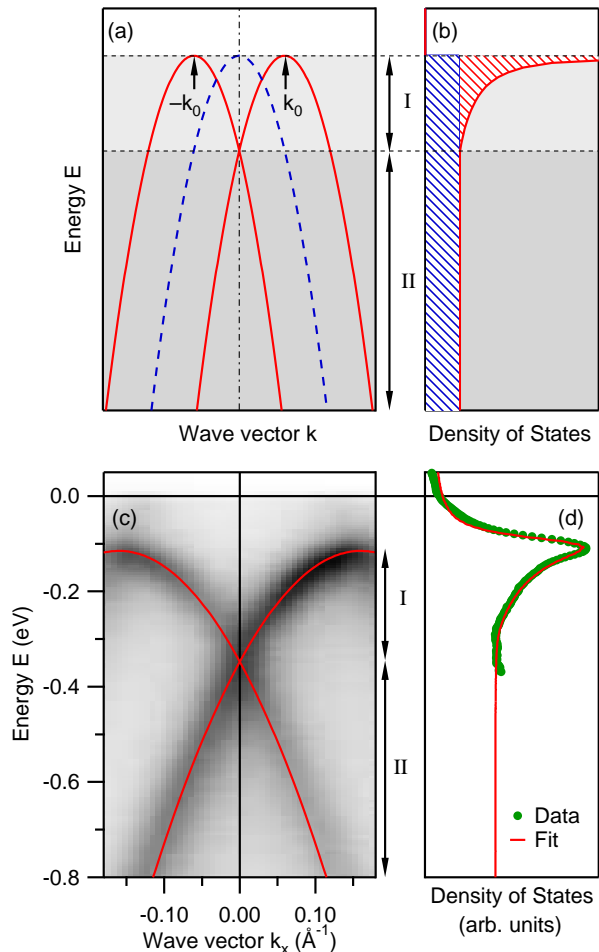


FIG. 3: (color online) Direct comparison of theory and experiment: (a) Calculated energy dispersion in the nearly free electron model with (red lines) and without (blue dashed line) spin-orbit coupling. (b) The corresponding density of states. (c) ARPES map of the band dispersion (red line) as a guide to the eye. (d) Local density of states measured by STS (green dots) with a fit from the nearly free electron model (red line).

Going from theory to experiment, the image in Fig. 3(c) shows the band structure measured by ARPES. The two red lines are the two shifted parabolic bands in the model with an effective mass $m^* = -0.4m_e$ as a guide to the eye. The extent of Region I is about 220 meV. Fig. 3(d) displays a dI/dV spectrum measured by STS (green dots) which is proportional to the LDOS of the sample. It shows a distinct peak which can be identified with the singularity in the calculated DOS in Fig. 3(b). The red line in Fig. 3(d) is a fit to the data by convoluting the DOS with a Lorentzian (40 meV full width at half maximum) to account for lifetime effects and experimental broadening. The fitted spin splitting parameter is $k_0 = 0.13 \text{ \AA}^{-1}$ in good agreement with ARPES.

The singularity at the band edge is a distinct feature of a spin-split band in a two-dimensional electron gas (2DEG). Therefore, the peak in the LDOS introduces a useful method

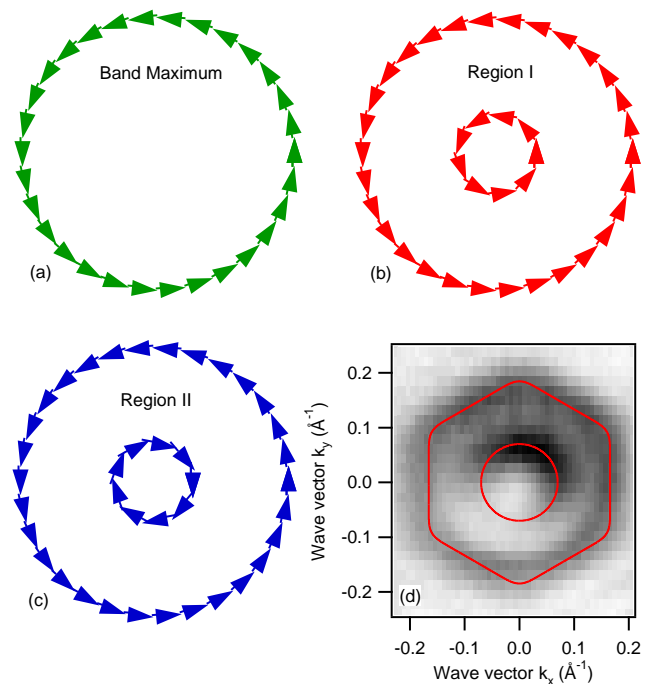


FIG. 4: (color online) Directions of spin rotation of the bands according to the nearly free electron model at the band maximum (a), in Region I (b), and in Region II (c). (d) Constant energy slice of the spin split bands in Region I at an energy of -180 meV measured by ARPES. The red lines indicate the contours of the energy bands as a guide to the eye.

for identifying the spin-splitting of energy bands by STS. It could not be observed in, for example, the Au(111) surface state because there the splitting is not as pronounced. If the width of Region I, determined by k_0 , is too narrow, broadening effects immediately dampen the singularity which will only appear as a step in the LDOS [13]. However, the asymmetric singularity may cause a small shift of the leading edge as well as a steeper slope. On the other hand, standing waves in dI/dV maps are often inconclusive in determining the spin splitting of a 2DEG because electrons with opposite spin do not interfere [12].

The spin orientation calculated from the spin-orbit Hamiltonian H_{SOC} is displayed schematically in Fig. 4(a)-(c) for three different energies, at the band maximum, within Region I, and within Region II. The spins lie within the plane of the surface where the sense of rotation depends on the direction of the electric field. At the band maximum only one constant energy contour is visible (we assume a counterclockwise spin orientation). Within Region I two contours of the same spin orientation can be associated to the inner and the outer branches of the energy bands. Crossing over to Region II the inner contour changes its sense of spin rotation. This scenario is different from what has been previously observed in spin-split bands where only Region II is observable experimentally [7, 11]. The large spin-splitting in the bismuth/silver surface alloy provides access to Region I with a qualitatively different spin configuration. The constant energy image in

Fig. 4(d) measured by ARPES shows two concentric contours at an energy of -180 meV, which is well within Region I. The inner contour is nearly circular, while the outer one is hexagonal due to its stronger interaction with the lattice potential. Qualitatively, however, the picture described in Figs. 4(a)-(c) concerning the spin-rotation holds true for the bismuth/silver surface alloy.

It is interesting to note that in the present system the high-Z element is not the substrate but the doping material. Moreover, neither clean Ag(111) ($k_0 = 0.004 \text{ \AA}^{-1}$) [17] nor the pristine Bi(111) surfaces ($k_0 \approx 0.05 \text{ \AA}^{-1}$) [18] exhibit such a strong spin splitting effect. We conclude that the formation of a surface alloy where adatoms are integrated in the top-most surface layer can lead to a strong enhancement of the effect. Model calculations give insight into this problem [12], but clearly first principle calculations are required to better understand the spin-dependent band structure in such interfaces as a function of chemical and structural parameters.

The giant spin-splitting observed in the Bi/Ag(111) surface alloy is not a unique phenomenon particular to this combination of materials but rather a property of a new class of materials. In particular, experiments on the Pb/Ag(111) surface alloy have shown an almost equally large spin-splitting with the

band maximum in the unoccupied states. This suggests that tuning of the Fermi level across the spin-split bands could be achieved by doping the bismuth/silver alloy with lead atoms. Preliminary work, which we have done, supports this idea. The ability of tuning the Fermi level through the different regions of the spin-split bands will offer an ideal playground to test fundamental ideas.

On a broader perspective, surface alloys could be tailored to specific applications. Ordered thin films of silver on a silicon surface have already been grown successfully [19]. Extending this to the present study, spin-split bands in a surface alloy on a semiconductor substrate becomes a real possibility with exciting perspectives in spintronics. Applying the spin-splitting parameters of the bismuth/silver alloy to the problem of the spin transistor, we find for the spin precession that a phase difference of $\Delta\theta = \pi$ is reached after a distance of $L = \Delta\theta/k_0 = 2.6 \text{ nm}$ [2], which is about two orders of magnitude smaller than for a semiconductor.

We gratefully acknowledge discussions with D. Malterre and H. Brune. C.R.A. acknowledges funding from the Emmy-Noether-Program of the Deutsche Forschungsgemeinschaft. The work at the EPFL was supported by the Swiss National Science Foundation through the MaNEP NCCR.

-
- [1] S. A. Wolf *et al.*, *Science* **294**, 1488 (2001).
 - [2] S. Datta and B. Das, *Appl. Phys. Lett.* **56**, 665 (1990).
 - [3] T. Koga, J. Nitta, H. Takayanagi, and S. Datta, *Phys. Rev. Lett.* **88**, 126601 (2002).
 - [4] J. I. Ohe, M. Yamamoto, T. Ohtsuki, and J. Nitta, *Phys. Rev. B* **72**, 041308(R) (2005).
 - [5] J. Henk, A. Ernst, and P. Bruno, *Phys. Rev. B* **68**, 165416 (2003).
 - [6] Y. A. Bychkov, E. I. Rashba, *JETP Lett.* **39**, 78 (1984).
 - [7] S. LaShell, B.A. McDougall, and E. Jensen, *Phys. Rev. Lett.* **77**, 3419 (1996).
 - [8] E. Rotenberg, J. W. Chung, and S. D. Kevan, *Phys. Rev. Lett.* **82**, 4066 (1999).
 - [9] M. Hochstrasser, J. G. Tobin, E. Rotenberg, and S. D. Kevan, *Phys. Rev. Lett.* **89**, 216802 (2002).
 - [10] O. Krupin *et al.*, *Phys. Rev. B* **71**, 201403(R) (2005).
 - [11] J. Henk, M. Hoesch, J. Osterwalder, A. Ernst, and P. Bruno, *J. Phys.: Condens. Matter* **16**, 7581 (2004).
 - [12] L. Petersen, and P. Hedegård, *Surf. Sci.* **459**, 49 (2000).
 - [13] J. Klier *et al.*, *Science* **288**, 1399 (2000).
 - [14] E. I. Rashba, *Phys. Rev. B* **68**, 241315(R) (2003).
 - [15] L. W. Molenkamp, G. Schmidt, and G. E. W. Bauer, *Phys. Rev. B* **64**, 121202(R) (2001).
 - [16] P. R. Hammar and M. Johnson, *Phys. Rev. Lett.* **88**, 66806 (2002).
 - [17] D. Popović *et al.*, *Phys. Rev. B* **72**, 045419 (2005).
 - [18] Yu. M. Koroteev *et al.*, *Phys. Rev. Lett.* **93**, 046403 (2004).
 - [19] e. g. M. Katayama, R. S. Williams, M. Kato, E. Nomura, and M. Aono, *Phys. Rev. Lett.* **66**, 2762 (1991).